# Target Plasma Formation for Magnetic Compression/Magnetized Target Fusion

I. R. Lindemuth, R. E. Reinovsky, R. E. Chrien, J. M. Christian, C. A. Ekdahl, J. H. Goforth, R. C. Haight, G. Idzorek, N. S. King, R. C. Kirkpatrick, R. E. Larson, G. L. Morgan, B. W. Olinger, H. Oona, P. T. Sheehey, J. S. Shlachter, R. C. Smith, L. R. Veeser, B. J. Warthen,* and S. M. Younger

*Los Alamos National Laboratory, Los Alamos, New Mexico 87545*

V. K. Chernyshev, V. N. Mokhov, A. N. Demin, Y. N. Dolin, S. F. Garanin, V. A. Ivanov, V. P. Korchagin, O. D. Mikhailov, I. V. Morozov, S. V. Pak, E. S. Pavlovskii, N. Y. Seleznev, A. N. Skobelev, G. I. Volkov, and V. A. Yakubov

*All-Russian Scientific Research Institute of Experimental Physics, Arzamas-16, Russia*

(Received 18 May 1995)

Experimental observations of plasma behavior in a novel plasma formation chamber are reported. Experimental results are in reasonable agreement with two-dimensional magnetohydrodynamic computations suggesting that the plasma could subsequently be adiabatically compressed by a magnetically driven pusher to yield 1 GJ of fusion energy. An explosively driven helical flux compression generator mated with a unique closing switch/opening switch combination delivered a 2.7 MA, 347 $\mu$s magnetization current and an additional 5 MA, 2.5 $\mu$s electrical pulse to the chamber. A hot plasma was produced and $10^{13}$ D-T fusion reactions were observed.

PACS numbers: 52.50.Lp, 52.40.Hf, 52.55.Ez, 52.65.Kj

Magnetic compression/magnetized target fusion (MAGO/MTF) is an area of fusion research that is intermediate between magnetic fusion energy (MFE) and inertial confinement fusion (ICF) in time and density scales. This concept has been pursued independently in Russia as MAGO (magnitnoye obzhatiye, or magnetic compression) [1,2] and in the U.S. [3,4]. MAGO/MTF uses a pusher-confined, magnetized, preheated plasma fuel within a fusion target. The magnetic field suppresses losses by electron thermal conduction in the fuel during the target implosion heating process. Reduced losses permit adiabatic compression of the fuel to ignition temperatures even at low (e.g., 1 cm/$\mu$s) implosion velocities. Previous work relevant to MAGO/MTF includes, but is not limited to, work in imploding liner fusion, impact fusion, and electron-beam driven "phi" targets. In some embodiments, MAGO/MTF is similar to the "staged $z$ pinch" [5], although the latter requires vacuum magnetic isolation of the fuel from the imploding liner, requires the inner surface of the imploding liner to retain adequate symmetry down to a final radius that is 1/2000 of its initial radius, and assumes stability of the fuel fiber (in contrast to previous experience [6]). In MAGO/MTF, the convergence ratio of the pusher is the same as the fuel, and in quasispherical geometries may potentially be less than 10, depending upon the initial temperature of the fuel and the adiabaticity of the implosion.

MAGO/MTF has not been extensively pursued, in part because of the challenges associated with developing and mating the two elements of an MTF system: (a) a target implosion system; and (b) a means of preheating and magnetizing the thermonuclear fuel prior to implosion.

A capacitor-bank-powered, magnetically driven implosion of a quasispherical shell, conceptually appropriate for a MAGO/MTF target pusher, has recently been reported [7]. The advent of 200-MJ-class disk flux compression generators [8,9] make it possible to consider direct magnetic implosion [2] of fusion targets to ignition conditions in an energy-velocity space simply inaccessible by any other laboratory means [10]. Such energy-rich sources appear ideal for MAGO/MTF, and consequently for a demonstration of fusion ignition, without a major capital investment in driver technology.

In this paper we report the results of experiments exploring a scheme [11–13] for forming a hot, magnetized plasma possibly suited for subsequent implosion in a MAGO/MTF context. The experiment described here used a copper plasma formation chamber shown in Fig. 1. The outer radius of the plasma volume was 10 cm. The overall length of the plasma volume was 16.6 cm. The

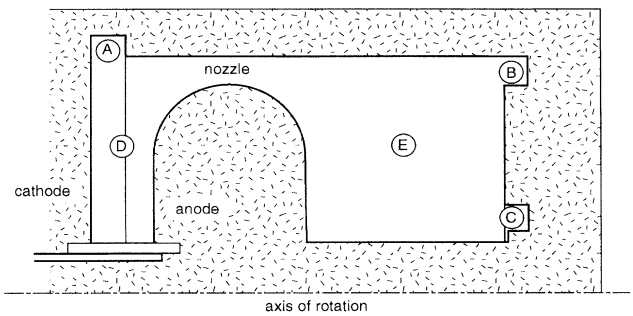


FIG. 1. The plasma formation chamber; points $A$, $B$, and $C$ indicate the location of inductive probes; points $D$ and $E$ indicate chordal lines of sight for plasma laser interferometry.

0031-9007/95/75(10)/1953(4)$06.00  

lengths of the left-hand and right-hand sections of the chamber were 2.6 and 8 cm, respectively. The nozzle opening was 1.2 cm. The chamber was initially filled with 10 Torr of 50% deuterium, 50% tritium gas seeded with 0.01% neon for diagnostic purposes. The chamber behavior was computationally modeled using two-dimensional magnetohydrodynamic techniques [14,15].

The chamber was powered by an explosively powered high-gain helical flux compression generator. Using a combination of explosively operated closing and opening switches, the pulse power system delivered a slowly rising pulse of electrical current to magnetize the gas followed by a rapidly rising pulse to drive the discharge. The measured chamber input current is shown in Fig. 2, curve *a*. At 347 $\mu$s ($t_0$), 2.7 MA were delivered to the chamber and magnetic probes interior to the chamber probe confirm that all of the initial, slowly rising current was carried in the chamber walls, encircled the gas volume, and provided an initial, "bias" magnetic field. Upon operation of the opening switch at 347 $\mu$s, the current flowing to the input of the chamber increased to 7.5 MA in 2.5 $\mu$s with a peak $dI/dt$ of approximately 4 MA/$\mu$s. Inductive probe measurements indicated that the rapidly rising resistance of the opening switch created a voltage sufficient to induce electrical breakdown somewhere within the gas in the chamber.

Figure 2 shows the measured (curve *b*) and computed (curve *c*) signals from an inductive probe located at point *A* of Fig. 1. For approximately 1.3 $\mu$s, the signal measured by the probe (curve *b*) closely followed the chamber input current (curve *a*). At 1.3 $\mu$s, the probe signal (curve *b*) became almost constant, while the chamber current (curve *a*) continued to rise, indicating the conduction of current somewhere between the insulator and the probe. According to the computations, this current drove an inverse *z* pinch in the left-hand side of the chamber. At 1.5 $\mu$s, the probe signal deviated noticeably from the input current, and at about 1.8 $\mu$s a series of oscillations with a peak-to-peak amplitude of approximately 0.75 MA was observed, indicating the arrival of compression waves in the vicinity of the probe and subsequent reflections from the chamber wall and the magnetic piston.

Until 2.3 $\mu$s, the measured and computed probe signals at location *B* increased only slightly from the initial 2.7 MA and were significantly less than the chamber input current, indicating that most of the rapidly rising input current flowed from the central anode to the outer chamber wall between probes *A* and *B*. This approximately radial current drove a shock wave into the right-hand side of the chamber. At approximately 2.3 $\mu$s, the experimental probe at location *B* showed the onset of oscillations of approximately 2 MA, indicating the arrival of a current sheath in the vicinity of the probe.

The inductive probe at point *C* showed a similar slow rise for about 2.4 $\mu$s, then an approximately monotonic increase at a rate of approximately 2 MA/$\mu$s. The slow initial rise in the probes at *B* and *C* was due to compression of the initial magnetization flux by the conducting gas piston driven by the current in the nozzle. Even as late as 4 $\mu$s, the probe signal value at *C* did not reach the full input current, indicating current flow from the central electrode to the right-hand wall between probes *B* and *C*.

Figure 3 shows the results of laser interferometry along chord *D* in Fig. 1 in the left-hand section. Curve *a* shows an abrupt increase in line-averaged electron density at 1.2 $\mu$s, indicating arrival of the radially expanding inverse *z*-pinch plasma sheath. The density reached a

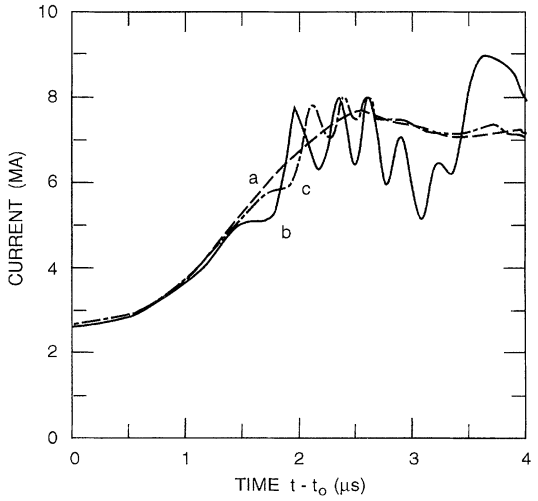


FIG. 2. Inductive probe signals ($t_0$ = 347 $\mu$s): (a) chamber input current; (b) current measurement at location *A* of Fig. 1; (c) computation for location *A*.

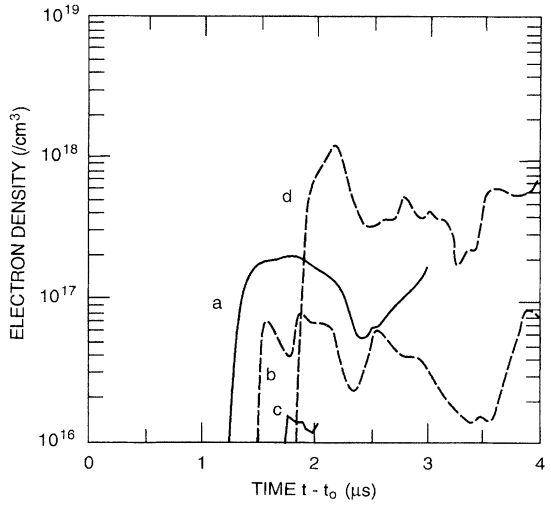


FIG. 3. Chordal line-of-site interferometric line-averaged electron density: (a) left-hand section of chamber; (b) computation for left-hand section; (c) right-hand section; (d) computation for right-hand section.

peak value of approximately $2.2 \times 10^{17}/\text{cm}^3$ and by 2.5 $\mu$s decreased to a value $5 \times 10^{16}/\text{cm}^3$. Because the initial fill density, if fully ionized, is $7 \times 10^{17}/\text{cm}^3$, the peak value of curve *a* indicates that the inverse pinch was not fully ionizing. The decrease in density was followed by an increase for about 0.5 $\mu$s, at which time the quadrature signals of the interferometer became uninterpretable.

An interferometric measurement along chord *E* in the right-hand chamber section returned useful data for only about 100 ns after the appearance of plasma in its line of sight (Fig. 3, curve *c*), indicating the time of plasma appearance at 1.7 $\mu$s. The computations (curve *d*) then show a rapid rise to $1.25 \times 10^{18}/\text{cm}^3$, a subsequent drop, and then oscillatory behavior. The first peak indicates that the gas was fully ionized by the compression wave driven from the nozzle and the subsequent behavior indicates plasma compression towards the axis at smaller radius than the chordal line of sight.

Neutron activation and time-of-flight measurements indicated the production of $1 \times 10^{13}$ 14.1 MeV neutrons from the deuterium-tritium fusion reaction. A peak reaction rate of $3 \times 10^{13}$ neutrons per $\mu$s with a FWHM of 300 ns was observed. The peak reaction rate occurred at 3.1 $\mu$s. The one-temperature ($T_i = T_e$) computations reported in this paper also give a neutron peak at approximately the same time with a similar pulse width. However, the computed total yield is approximately 2 orders of magnitude too low. Two-temperature ideal gas computations (separate $T_i, T_e$; initially $T_i = T_e = 2$ eV) more closely match the observed yield but do not match the inductive and interferometric measurements because of the high initial electrical conductivity of the entire gas within the chamber.

The computations indicate that the gas that was originally in the left-hand section is compressed by the inverse pinch and accelerated through the nozzle. Upon exiting the nozzle, the fast-moving (20–100 cm/$\mu$s) plasma contacts the compressed plasma of the right-hand section, and its kinetic energy is converted to thermal energy. Some plasma (<5%) reaches temperatures higher than 1 keV, and it is from this plasma that the thermonuclear neutrons originate. The two-temperature computations suggest that the ion temperature of the neutron-producing plasma became significantly higher than the electron temperature.

A signal from one of four filtered silicon x-ray detectors is shown in Fig. 4 (curve *a*). Curve *b* in Fig. 4 is the computed time history of the total hydrogenic continuum radiation above 700 eV—the approximate lower cutoff of the detector—for approximately the same line of sight viewed by the detector. The x-ray signals indicate the arrival of hot ($T > 100$ eV) plasma within the detector line of sight. The measured signals persist until at least 7 $\mu$s giving reason to be optimistic that such a plasma may be suitable for compression on time scales of 5–10 $\mu$s.

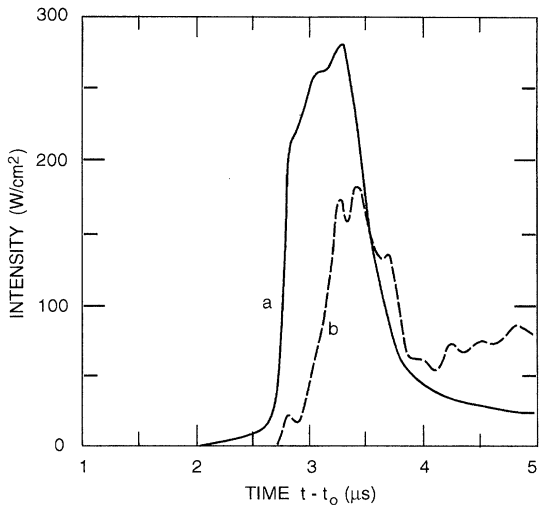


FIG. 4. X-ray signals for right-hand section of chamber, axial view at 6 cm radius: (a) filtered silicon diode detector; (b) computed hydrogenic continuum above 700 eV.

Because of the complex detector geometry, there is some arbitrariness in the analysis leading to the computed signal of Fig. 4, curve *b*, and the analysis does not take into account the contributions of the 0.01% neon and the filter transmission function. A more detailed computational analysis taking into account line and continuum radiation and the transmission function is in progress.

Like other high-energy-density gas discharge configurations, it would be expected that the plasma would at some time show contamination by wall material (e.g., copper) and that insulator constituents could enter the chamber behind the plasma and possibly mix with the hot plasma during the late times. Spectral measurements performed on the experiment reported here and on earlier experiments have proven inconclusive. An optical multichannel analyzer (OMA) viewing the insulator for a 500 ns window beginning at 1.5 $\mu$s showed emitted radiation characteristic of the insulator material as expected, but the qualitative interpretation of the OMA data indicates that the density of insulator material was small. A streak spectrograph viewing the left-hand chamber at chord *D* of Fig. 1 showed the initiation of the $H_\beta$ line at approximately 2.5 $\mu$s but did not show indication of any nonhydrogenic species until 4 $\mu$s.

For time later than about 4 $\mu$s, i.e., after the very complex early-time plasma formation process, the computations show a surprisingly stationary plasma in the right-hand section of the chamber. The plasma can be roughly described as a diffuse, wall-confined *z* pinch. The plasma is approximately one dimensional, with plasma parameters such as density, temperature, and magnetic field varying only with radius. Average computed late-time (10 $\mu$s) plasma parameters are $n_e = 1.6 \times 10^{18}/\text{cm}^3$, $\rho =$

$6.7 \times 10^{-6}$ g/cm$^3$, $T = 130$ eV, $B = 240$ kG, $\beta = 0.3$, and $(\omega\tau)_e = 140$. In all diagnostics, the computations show an approximately 200 ns lag when compared to experiment. This lag is eliminated in computations driven by a slightly higher current that is within experimental error. The essential results of the computations are unchanged.

Results of survey spherical target computations [3] based upon the experimental mass (8.9 mg), average computed temperature and magnetic field, and an implosion kinetic energy of 65 MJ are summarized in Fig. 5. A region of unity gain (curve *b*) occurs for initial densities above about $10^{-6}$ g/cm$^3$ and initial velocities above approximately 0.2 cm/$\mu$s. Gains in excess of 10 (curve *a*) occur for densities and velocities approximately 2–3 times higher. A gain of 16, and a thermonuclear yield of 1 GJ, is predicted for a density of $6.7 \times 10^{-6}$ g/cm$^3$, a pusher implosion velocity of 2 cm/$\mu$s, and a maximum radial convergence of less than 20. The survey computations show that the 290 eV average temperature computed for an earlier, lesser diagnosed experiment can significantly reduce the convergence required and that approximately adiabatic compression can be expected for initial magnetic fields as low as 75 kG.

The survey results (Fig. 5) coupled with the two-dimensional computations suggest that a plasma suitable for subsequent implosion in a MAGO/MTF context has been produced in the experiment reported here. Further plasma formation experiments are required before the present plasma chamber can be confidently mated with an implosion system. Future experiments will emphasize characterization of the late time plasma behavior and will search for wall and insulator impurities that would degrade the implosion heating process by enhancing the radiation energy losses from the plasma. Although it is quite plausible that the present plasma chamber could be scaled to a smaller size, reducing the implosion energy required, existing high-explosive pulsed power devices [8,10] are sufficient to provide the 65 MJ of energy used in the survey computations of Fig. 5.

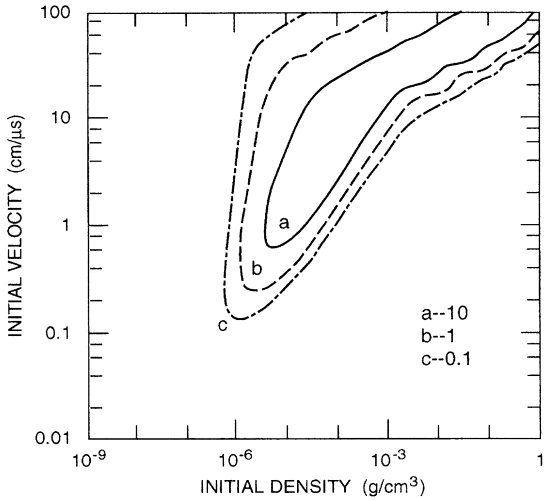


FIG. 5. Gain contours computed using model of [3]. Mass: 8.9 mg. Initial kinetic energy: 65 MJ. Minimum initial temperature: 130 eV. Initial magnetic field: 240 kG.

The experiment reported in this paper is one of several endeavors in the area of pulsed power and ultrahigh magnetic fields conducted as part of scientific collaboration between institutions in the United States and the Russian Federation, which have historically had the development of nuclear weapons as their major mission. This collaboration would not have been possible without the support and encouragement of many officials of the governments of Russia and the United States and many administrators and colleagues at the All-Russian Scientific Research Institute of Experimental Physics and the Los Alamos National Laboratory.

*Also at E.G. & G./EM, Los Alamos Operations, Los Alamos, NM 87545.

[1] Yu. B. Khariton *et al.,* Usp. Fiz. Nauk. **120**, 706 (1976) [Sov. Phys. Usp. **19**, 1032 (1976)].
[2] V. N. Mokhov *et al.,* Sov. Phys. Dokl. **24**, 557 (1979).
[3] I. R. Lindemuth and R. C. Kirkpatrick, Nucl. Fusion **23**, 263 (1983).
[4] R. C. Kirkpatrick, I. R. Lindemuth, and M. S. Ward, Fusion Technol. **27**, 201 (1995).
[5] H. U. Rahman, F. J. Wessel, and N. Rostoker, Phys. Rev. Lett. **74**, 714 (1995).
[6] P. T. Sheehey *et al.,* Phys. Fluids B **4**, 3698 (1992).
[7] J. H. Degnan *et al.,* Phys. Rev. Lett. **74**, 98 (1995).
[8] V. K. Chernyshev *et al.,* in *Megagauss Fields and Pulsed Power Systems,* edited by V. Titov and G. Shvetsov (Nova Science Publishers, New York, 1990).
[9] A. I. Pavlovskii *et al.,* in Ref. [8].
[10] R. E. Reinovsky, I. R. Lindemuth, and S. P. Marsh, in *Digest of Technical Papers: Proceedings of the VIII IEEE Pulsed Power Conference,* edited by R. White and K. Prestwich (Institute of Electrical and Electronics Engineers, New York, 1991).
[11] A. M. Buyko *et al.,* VANT Ser. Metodiki i Programmy Chislennogo Resheniya Zadach Matematicheskoi Fiziki **3**, 30 (1983).
[12] A. M. Buyko *et al.,* in *Digest of Technical Papers: Proceedings of the IX IEEE Pulsed Power Conference,* edited by K. Prestwich and W. Baker (Institute of Electrical and Electronics Engineers, New York, 1993).
[13] V. K. Chernyshev *et al.,* in *Megagauss Magnetic Field Generation and Pulsed Power Applications,* edited by M. Cowan and R. B. Spielman (Nova Science Publishers, New York, 1995).
[14] I. R. Lindemuth *et al.,* in Ref. [13].
[15] P. T. Sheehey *et al.,* in *Beams 94: 10th International Conference on High Power Particle Beams,* edited by W. Rix (National Technical Information Service, Springfield, VA, 1994).